Analytical Determination of Blockage Effects in a Perforated-Wall Transonic Wind Tunnel

E. M. Kraft* and C. F. Lo†
ARO, Inc., Arnold Air Force Station, Tenn.

Two analytical methods for determining the interference effects of a perforated wind-tunnel wall on the flow past a two-dimensional nonlifting airfoil at transonic speeds are presented. The first method approximates the flowfield with the linearized transonic small disturbance equation and the interference velocity is determined directly by Fourier transform techniques. This method is readily extended to axisymmetric flows. The second method solves the nonlinear transonic small disturbance equation including shock waves by an integral equation method which is shown to be an order of magnitude more rapid than existing numerical relaxation techniques. It is demonstrated by the integral equation solution that the correct shock location as compared to the free-air solution can be obtained by the proper selection of porosity. However, this optimum porosity is shown to be dependent on the Mach number and the airfoil configuration.

I. Introduction

INTERFERENCE effects on data obtained in wind tunnels caused by the inevitable constraints posed by the tunnel walls have been recognized ever since wind tunnels were originated. The introduction of ventilated wind tunnels has reduced greatly the magnitude of the wall effects. However, even in ventilated wind tunnels, wall interference corrections must be applied. Classical wall interference theory is based on linearized subsonic theory with compressibility effects accounted for by the Prandtl-Glauert scaling laws.[1,2] Linearized subsonic theory fails to predict the flowfield correctly, however, when local supercritical velocities occur. Consequently, a nonlinear or transonic theory must be used to describe the features of mixed subsonic-supersonic flows and formation of embedded shock waves. In this paper, the application of transonic theory to wind-tunnel flow situations is presented for supercritical subsonic flow past a nonlifting airfoil.

Prior to 1971, methods for detailed investigation of the transonic flow in wind tunnels including shock waves were not available. Applications of the linearized transonic theory at sonic velocities were made by Murasaki[3] for slotted- and perforated-wall wind tunnels and by Sandeman[4] for closed-wall tunnels. The ability of a choked wind tunnel to simulate closely the flow about a profile in an unbounded stream with sonic velocity at infinity is well established[5] and the investigations of Murasaki and Sandeman were performed to estimate the residual corrections required to give the unbounded sonic pressure distribution. Other solutions at sonic velocities where the governing equations conveniently reduce to the form of the parabolic heat equation have been obtained by Romberg[6] and Goodman.[7] Berndt[8] investigated the governing equations, boundary conditions, transonic similarity rules, and effects of tunnel wall boundary layers on wall interference. He also reviewed the work done on the application of transonic theory to subsonic and sonic wind-tunnel flows prior to 1964.

About 1970, numerical solutions to the transonic small-disturbance equation, using relaxation methods developed by Murman and Cole[9] and subsequent researchers, provided a new level of capability in transonic flow analyses. Bailey[10] examined the effects of wind-tunnel boundaries on a body of revolution and Murman,[11] Kacprzynski,[12] and Catheral[13] have considered interference effects on two-dimensional airfoils. Time-dependent methods for calculating transonic flow over two-dimensional airfoils in wind tunnels have been developed by Laval[14] and Laval and Erard.[15] More recently, Newman and Klunker[16] have extended the relaxation method in three dimensions to determine the interference effects on finite wings in rectangular tunnels.

The numerical methods provide an analysis for the flow around an airfoil in the wind tunnel but do not yield tunnel corrections directly. The free-air solutions have to be compared with the tunnel solution to obtain the tunnel corrections. Thus, analytical approaches to the problem are attractive since they can be used to determine directly the tunnel corrections without solving for the free-air flowfield. This paper is concerned with the development and application of two analytical methods for determining tunnel interference effects at transonic speeds. The first method is an approximate method concerned with solving the transonic linearized theory for flows less than sonic over two-dimensional airfoils and bodies of revolution in perforated-wall wind tunnels. The method provides a direct means for correcting the pressure distribution on the model but does not include tunnel effects on shock wave location which can be treated by the second method.

The second method presented in this paper is believed to be the first analytical approach to flow past airfoils in perforated-wall wind tunnels using the nonlinear transonic small-disturbance equation including embedded supersonic regions with shock waves. The solution is obtained by an integral equation method and is essentially equivalent to the numerical solutions using the relaxation method. The advantages of the integral method are, first, the linear and nonlinear contributions to wall interference can be isolated from the integral equation since it is a natural extension of the classical, linear subsonic solutions for wall interference. Secondly and most important, it requires, in general, an order of magnitude less computing time than the numerical methods.

II. Analysis

Transonic Small-Disturbance Equation

Transonic small-disturbance theory can be derived from the exact inviscid equations of fluid dynamics by considering the asymptotic limits of small perturbations in the velocity components and freestream velocity approaching sonic

Presented at the AIAA 9th Aerodynamic Testing Conference, Arlington, Texas, June 7-9, 1976 (in bound volume of conference papers, no paper number) submitted June 30, 1976; revision received Dec. 13, 1976.

Index categories: Aircraft Testing (including Component Wind Tunnel Testing); Subsonic and Transonic Flow.

*Research Engineer, PWT. Member AIAA.

†Supervisor, 4T Projects Branch, PWT. Member AIAA.

conditions (e.g., Ref. 17). For the present study it is assumed that the flow is two-dimensional, steady, and inviscid and that the fluid is a perfect gas. The transonic potential equation is then

$$\beta^2\Phi_{xx}-M_T^2(\gamma+1)\Phi_x\Phi_{xx}+\Phi_{yy}=0 \tag{1}$$

where $\beta^2=1-M_T^2$, M_T is the tunnel reference Mach number, and the potential Φ is the first-order perturbation from uniform freestream conditions. An expansion procedure in the primary variables[9] indicates that the flow is potential to the first two orders but that entropy production must be considered in higher orders. The nonlinear term in Eq. (1) yields an equation of mixed elliptic-hyperbolic type and allows the formation of embedded shock waves. The exponent for M_T in Eq. (1) is not unique and depends on the expansion procedure considered. A detailed discussion is given by Murman[11] and Krupp.[18]

Boundary Conditions

For a nonlifting airfoil the condition of tangential flow at the body surface with coordinates

$$y_{u,\ell}=\pm\tau F_x/2 \tag{2}$$

where u and ℓ refer to the upper and lower surfaces, respectively, τ is the thickness ratio, and $F(x)$ is the shape function of the airfoil. Equation (2) is applied on the mean surface of the airfoil at $y=0$.

The equation derived by Baldwin, et al.[19] is used to model the perforated wind-tunnel wall. Their homogeneous boundary condition is a linearized approximation to the viscous flow through a porous medium in which the average velocity normal to the wall is assumed to be proportional to the pressure drop Δp through the wall, namely

$$\Phi_x\pm(1/R)\Phi_y=0, \quad y=\pm h \tag{3}$$

where R is a porosity parameter defined by

$$R=\frac{-\partial\Phi/\partial y}{\partial\Phi/\partial x}=\frac{2V_n/U_T}{\Delta p/q_T} \tag{4}$$

where V_n is the velocity normal to the tunnel boundaries, U_T is the freestream velocity, and q_T is the freestream dynamic pressure. For convenience, a normalized porosity parameter, $Q=(1+\beta/R)^{-1}$, will be used for presentation of the results.

Various authors have challenged the validity of the linear porous wall boundary condition. However, Jacocks[20] recently has shown that in an average sense Eq. (3) is a reasonable representation of a porous wall. The difficulty in applying Eq. (3) is the determination of R. Jacocks has shown that R is not only sensitive to wall goemetry, Mach number, and Reynolds number, but also to the model induced pressure field and boundary-layer development on the wall. He suggests measuring flow variables near the wall and using these to specify the boundary conditions.

Finally, the tunnel test section is assumed to be sufficiently long that the axial perturbation velocity vanishes

$$\Phi_x\to 0 \quad \text{as} \quad x\to\pm\infty \tag{5}$$

The foregoing boundary conditions are shown schematically in Fig. 1.

Linearized Transonic Theory (LTT)

The linearized transonic theory (LTT) was first proposed by Oswatitsch[21] and later extended by Maeder and Wood.[22] In addition, Spreiter[23] introduced the method of local linearization by replacing part of the nonlinear term in a small region by a constant. A hybrid method of these theories will be used in the present approach. For convenience of tunnel blockage interference calculation, the transonic small-disturbance equation is written in terms of the axial velocity, $u=\partial\phi/\partial x$. Equation (1) is linearized by assuming ϕ_{xx} to be an average constant, $\bar{\phi}_{xx}$, over the airfoil, thus the linearized transonic equation is

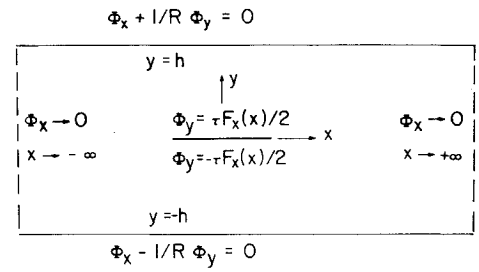

Fig. 1 Boundary conditions for nonlifting airfoil in a perforated wind tunnel.

$$\beta^2u_{xx}+u_{yy}=ku_x \tag{6}$$

where

$$k=(\gamma+1)M_T^2\Phi_{xx} \tag{7}$$

The corresponding boundary conditions for u are

$$u_y=\tau F_{xx}/2 \quad \text{at} \quad y=0 \tag{8}$$

$$u_x\pm(1/R)u_y=0 \quad \text{at} \quad y=\pm h \tag{9}$$

and

$$u=0, \qquad x\to\pm\infty \tag{10}$$

In order to solve the boundary-value problem posed in Eqs. (6-10), the Fourier transform technique is applied. In the transformed plane Eq. (6) becomes

$$\bar{u}_{yy}-\lambda^2\bar{u}=0 \tag{11}$$

where

$$\bar{u}(p,y)=(2\pi)^{-1/2}\int_{-\infty}^{\infty}u(x,y)e^{ipx}\mathrm{d}x \tag{12}$$

and

$$\lambda^2=\beta^2p(p-ik/\beta^2) \tag{13}$$

The transformed boundary condition at $y=0$ is

$$\bar{u}_y(p,0)=(2\pi)^{-1/2}\int_{-\infty}^{\infty}\frac{\tau}{2}F_{xx}e^{ipx}\mathrm{d}x=\frac{\tau}{2}f(p) \tag{14}$$

and at $y=+h$

$$-ip\bar{u}+(1/R)\bar{u}_y=0 \tag{15}$$

The solution in the transformed plane is

$$\bar{u}=\bar{u}_m-\frac{\tau f(p)}{2\lambda}\frac{(ip+\lambda/R)e^{-\lambda h}\cosh(\lambda y)}{[-ip\cosh(\lambda h)+\lambda/R\sinh(\lambda h)]} \tag{16}$$

where $\bar{u}_m=-[\tau f(p)/2\lambda]e^{-\lambda y}$ is the solution for the free-air flow in the transformed plane. The detailed solution for u_m in the physical plane can be obtained by the Fourier inversion formula and the details are given by Maeder and Wood.[22] The interference velocity induced by the tunnel wall $\bar{u}_i$ is determined directly from Eq. (16):

$$\bar{u}_i=\bar{u}-\bar{u}_m=-\frac{\tau f(p)}{2\lambda}\frac{(ip+\lambda/R)e^{-\lambda h}\cosh(\lambda y)}{[-ip\cosh(\lambda h)+\lambda/R\sinh(\lambda h)]} \tag{17}$$

The interference velocity in the physical plane is obtained by the inversion formula (see Ref. 24 for details) in the form

$$u_i(x,y)=u_i[\alpha,R,h,F(x);x,y] \tag{18}$$

The interference velocity may be calculated easily from Eq. (18) once the parameter, α, related to the acceleration parameter by

$$\alpha = k/2 = (\gamma+1)M_T^2\tilde{\Phi}_{xx}/2 \tag{19}$$

is determined. To determine α one assumes that it consists of two parts

$$\alpha = \alpha_1 + \alpha_2 \tag{20}$$

where α_1 is induced by the model in free air and α_2 is induced by the presence of the tunnel wall. The acceleration parameter α_1 is derived from the velocity solution in the free-air case.[22] In the manner of the local linearization method,[23] α_2 is allowed to vary along the streamwise direction in the final determination of the acceleration parameter. The acceleration parameter induced by the tunnel walls α_2 is determined by differentiating Eq. (18) with respect to x

$$\alpha_2 = \partial u_i/\partial x = (\gamma+1)M_T^2 G(\alpha,x)/2\beta^2 \tag{21}$$

where $G(\alpha,x)$ is defined in Ref. 24. The acceleration parameter α_1 is a constant averaged over the model, but α_2 is a local acceleration dependent on x. An iteration scheme is required to determine u_i, α_1, and α_2 from Eqs. (18, 20, and 21). The interference pressure coefficient is expressed as $C_{p_i} = -2u_i$.

The LTT method yields directly the interference perturbation velocity and, because of the simplicity introduced by the linearization, the method easily can be extended to a circular tunnel. However inherent to the LTT method are restrictions on treatment of shock waves in the flowfield. Although approximate methods for simulating the effects of shock waves have been incorporated in the LTT method in free air,[25] a fully nonlinear theory is required to evaluate adequately the effects of the tunnel boundaries on shock wave location. Such a technique is discussed in the next section

Integral Equation Method (IEM)

The governing Eq. (1) and boundary conditions, Eqs. (2) and (3) may be cast in similarity form by introducing transformations for Φ and y. These transformations yield similarity rules and illustrate some important differences between linearized subsonic theory and nonlinear transonic theory. A discussion of the transonic scaling laws for wall interference is given by Berndt[8] and Murman.[11] Introducing the transformations

$$\phi = (M_T/\tau)^{2/3}\Phi \tag{22}$$

$$\bar{y} = (M_T^{2/3}\tau^{1/3})y \tag{23}$$

then Eq. (1) becomes

$$K\phi_{xx} - (\gamma+1)\phi_x\phi_{xx} + \phi_{\bar{y}\bar{y}} = 0 \tag{24}$$

where

$$K = \beta^2/M_T^{4/3}\tau^{2/3} \tag{25}$$

The K is the transonic similarity parameter which cannot be eliminated from the problem by further transformation. Furthermore, the powers of M_T in Eqs. (22, 23, and 25) are not unique and various authors[11,17] use other values to improve the accuracy of the theory for Mach numbers other than unity. The body boundary condition becomes

$$(\phi_{\bar{y}})_{u,\ell} = \pm F_x \tag{26}$$

and the tunnel wall boundary condition is

$$\phi_x \pm (1/\tilde{R})\phi_{\bar{y}} = 0 \quad \text{on} \quad \bar{y} = \pm\tilde{T}/2 \tag{27}$$

where

$$\tilde{R} = M_T^{-2/3}\tau^{-1/3}R \tag{28}$$

$$\tilde{T} = 2M_T^{2/3}\tau^{1/3}h/c \tag{29}$$

For purposes of data presentation, it is convenient to introduce a normalized porosity parameter, $\tilde{Q} = (1+1/\tilde{R})^{-1} = (1+\beta/(K)^{1/3}R)^{-1}$. With the transonic scaling used, a flow in a wind tunnel at Mach number M_T past a body of thickness τ is similar to another flow M_{T_2} and τ_2, only if two flows have the same values of K, $\tilde{R}$, and $\tilde{T}$.

To form a complete system of equations, the shock-jump conditions which may be derived from the full Rankine-Hugoniot relations must be appended to Eq. (24). However, an important feature of the transonic small-disturbance equations is that the shock-jump conditions are contained in the system when they are written in conservative form. To the order considered, the shock-jump relations are

$$\langle K\Phi_x - [(\gamma+1)/2]\phi_x^2\rangle(d\bar{y})_s - \langle\Phi_{\bar{y}}\rangle(dx)_s = 0 \tag{30a}$$

$$\langle\phi_x\rangle(dx)_s + \langle\Phi_{\bar{y}}\rangle(d\bar{y})_s = 0 \tag{30b}$$

where $\langle f\rangle = f^2 - f^1$, the superscripts 1 and 2 referring to the upstream and downstream sides of the shock, respectively, and the subscript s indicates an element in the shock.

The solution to the preceding set of equations is determined by an intergral equation which is equivalent to the original system of differential equations and boundary conditions, and is in fact valid whether or not shock waves are present in the flow. This integral equation is based on combining the scaled irrotationality condition with Eq. (24) and separating off the linear part of the operators to form the vector system

$$Lq = \begin{pmatrix} u_x + v_{\bar{y}} \\ u_{\bar{y}} - v_x \end{pmatrix} = \begin{pmatrix} (u/2)_x^2 \\ 0 \end{pmatrix}$$

where for convenience the system has been further normalized by $\bar{x} = x$, $\bar{y} = (K)^{1/2}\bar{y}$, $u = (\gamma+1)\partial\phi/\partial x/K$, and $v = (\gamma+1)\partial\phi/\partial y/K^{3/2}$ The integral equation is constructed by in-

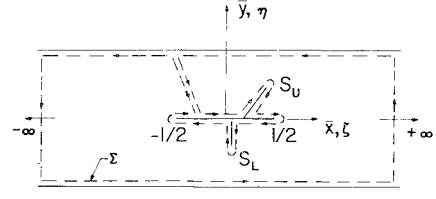

Fig. 2 Region of application of integral relation.

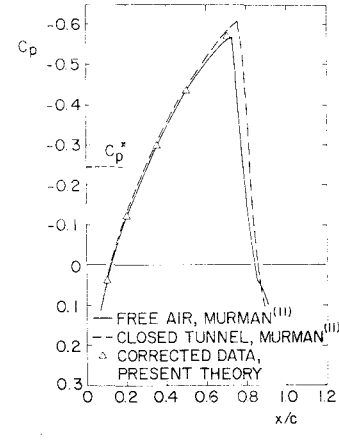

Fig. 3 Pressure coefficient on a 6% biconvex airfoil at $M_T = 0.875$ and $h/c = 3.4$.

troducing the vector function $Q=(U(x,y;\xi,\eta),\ V(x,y,\xi;\eta))$ and applying Green's theorem

$$\iint_A (Q\cdot Lq+q\cdot LQ)\mathrm{d}\xi\mathrm{d}\eta=\int_\Sigma \{(uU-vV)\mathrm{d}\eta-(Uv+Vu)\mathrm{d}\xi\} \tag{32}$$

to the region shown in Fig. 2. In applying Green's theorem, the shock jumps are treated as discontinuities, but when the jump conditions are taken into account, the shock waves disappear from the final integral quation. In order to make the line integrals along the tunnel boundaries vanish it is assumed that

$$U\pm(\beta/R)V=0, \qquad \bar{y}=\pm\beta h/c=\pm\lambda\beta \tag{33}$$

and $U,\ V\to 0$ as $|\bar{x}|\to\infty$. The final result for the axial perturbation velocity is

$$u(\bar{x},\bar{y})=\int_{-1/2}^{1/2}[U_v]_{\eta=0}\mathrm{d}\xi-\int_{-\infty}^{\infty}\int_{-\lambda\beta}^{\lambda\beta}\frac{u^2}{2}U\xi\mathrm{d}_\eta\mathrm{d}\xi$$
$$+\int_{-\lambda\beta}^{\lambda\beta}\left(\lim_{\epsilon\to 0}\ U\frac{u^2}{2}\Big|_{\bar{x}-\epsilon}^{\bar{x}+\epsilon}\right)\mathrm{d}\eta \tag{34}$$

where $\lambda=h/c$ and $[\ ]_{\eta=0}=f(\eta=+0)-f(\eta=-0)$. For a symmetric nonlifting airfoil, the influence function U represents the real part of the complex velocity $W(z,\zeta)$ at $z=\bar{x}+i\bar{y}$ caused by a unit source at $\zeta=\xi+i\eta$ between the perforated walls. The term $W(z,\zeta)$ is determined by representing the perforated walls with an image system such as the one developed by Mokry.[26] The final equation for the axial perturbation velocity at the airfoil surface, $y=0$, is

$$u(\bar{x},0)=\hat{u}(\bar{x},0)+[u^2(\bar{x},0)/2]-I(\bar{x}) \tag{35}$$

where the first term on the right-hand side is the linear solution for flow past an airfoil in a perforated-wall wind tunnel and is given by

$$\hat{u}(x,0)=\hat{u}_\infty(\bar{x})+\hat{u}_i(\bar{x})=\frac{1}{\pi}\int_{-1/2}^{1/2}\frac{F_\xi(\xi)}{x-\xi}\mathrm{d}\xi$$
$$+\int_{1/2}^{1/2}\frac{F_\xi(\xi)}{4\lambda\beta}\left[\frac{-e^{\kappa\xi_0}}{e^{\xi_0}+1}+\frac{e^{\kappa\xi_0}}{e^{\xi_0}-1}-\frac{1}{2\xi_0}\right]\mathrm{d}\xi \tag{36}$$

where $\xi_0=\pi(\bar{x}-\xi)/2\lambda\beta$ and $\kappa=(2/\pi)\arctan(R/\beta)$ is the porosity parameter. The first term of Eq. (36) is the linear free-air solution and the second term is the linear interference velocity induced by the perforated walls. The last term of Eq. (35) is the double integral

$$I(\bar{x})=\int_{-\infty}^{\infty}\int_{-\lambda\beta}^{\lambda\beta}\frac{u^2(\xi,\eta)}{2}\frac{\partial}{\partial\xi}R\Big\{S_1(\bar{x},0;\zeta)$$
$$+S_2(\bar{x},0;\zeta)+\frac{1}{2\pi(x-\zeta)}\Big\}\mathrm{d}\eta\mathrm{d}\xi \tag{37}$$

where

$$S_1(z;\zeta)=\frac{-1}{4\lambda\beta}\frac{\exp[\pi\kappa(z-\zeta^*)/2\lambda\beta]}{\exp[\pi(z-\zeta^*)/2\lambda\beta]+1} \tag{38}$$

and

$$S_2(z;\zeta)=\frac{1}{4\lambda\beta}\frac{\exp[\pi\kappa(z-\zeta)/2\lambda\beta]}{\exp[\pi(z-\zeta)/2\lambda\beta]-1}-\frac{1}{2\pi(z-\zeta)} \tag{39}$$

The * superscript indicates a complex conjugate. For sufficiently low Mach numbers, the u^2 terms become vanishingly small, and Eq. (35) reduces to $u=\hat{u}$ which is the linear subsonic solution.

Equation (35) is a nonlinear Fredholm integral equation of the same form as the classical Oswatisch[27] integral equation for transonic flow past unconfined airfoils and can be solved numerically by an iteration process. The double integral $I(\bar{x})$ is reduced to a single integral by assuming that the velocity decays in the transverse direction in the manner

$$u(\bar{x},\bar{y})=u(\bar{x},0)e^{-\bar{y}/r(\bar{x})} \tag{40}$$

where $r(\bar{x})$ is chosen so that the irrotationality condition is satisfied on the airfoil to yield

$$r(\bar{x})=-u(\bar{x},0)/(\partial u/\partial\bar{y})_{\bar{y}=0} \tag{41}$$

Norstrud[28] examined several functional forms for the decay parameter $r(\bar{x})$ and established that $I(\bar{x})$ is essentially insensitive to the details of the velocity decay. In addition, Nixon[29] argued that the disparity between the early integral equation solutions and recent numerical solutions was caused

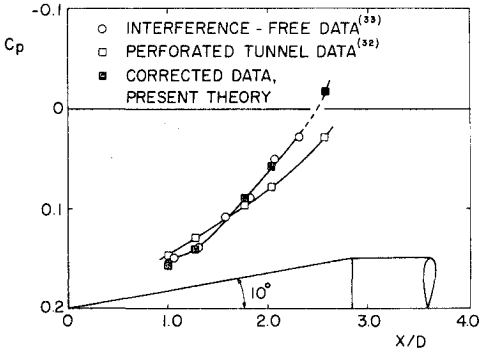

Fig. 4 Pressure coefficient on a 1.47% blockage cone-cylinder at $M_T=0.95$.

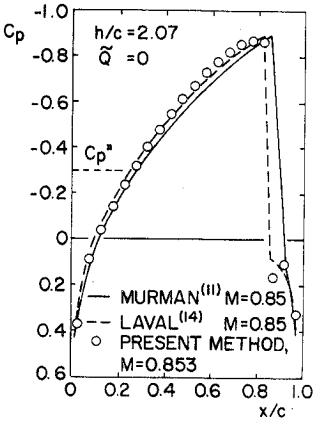

Fig. 5 Pressure coefficient on an 8.4% biconvex airfoil in a closed wind tunnel.

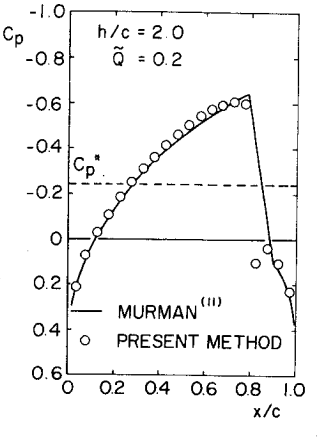

Fig. 6 Pressure coefficient on a 6% biconvex airfoil in a perforated wall tunnel at $M_T=0.875$.

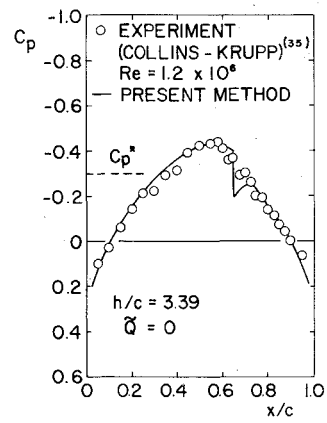

Fig. 7 Pressure coefficient on a 6% biconvex airfoil in a closed wind tunnel at $M_T = 0.857$.

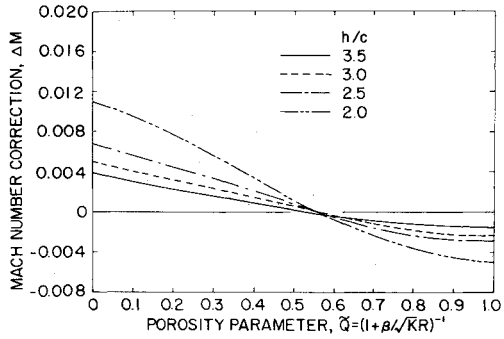

Fig. 8 Mach number correction at $M_T = 0.87$ on a 6% biconvex airfoil at various porosities.

by the assumption of Eq. (40). He circumvented this assumption by numerically integrating across several streamwise strips to produce better correlation with the numerical solutions. However, in Ref. 30, a systematic study of $r(\bar{x})$ indicated that excellent correlation between the integral equation method and numerical methods could be obtained, at least in unconfined flow, by only varying r with $\bar{x}$, if the radius of curvature of the airfoil varied significantly with $\bar{x}$ (as near the leading edge of a blunt-nosed airfoil).

For the numerical solution of Eq. (35), it is necessary to subdivide the integration over the airfoil into, say N, discrete integration intervals. Furthermore by replacing S_1 and S_2 by equivalent series of Euler and Bernoulli polynominals and using Eq. (40), the double integral $I(\bar{x})$ can be integrated analytically over each interval (see Ref. 30 for details) to yield a system of N nonlinear algebraic equations:

$$u_j = \hat{u}_j + \frac{u_j^2}{2} - \sum_{k=1}^{N} \frac{\hat{u}_k^2}{2} \epsilon_{jk}, \qquad j = 1,2,\ldots,N \tag{42}$$

where ϵ_{jk} are the elements of an influence matrix determined by integrating $I(\bar{x})$ over each subinterval. An expression for ϵ_{jk} is given in Ref. 30.

It is possible to rearrange Eq. (35) or (42) to directly provide an expression for the interference perturbation velocity, say u_i, but, for purposes of comparison with other solutions of the transonic small-disturbance equation, Eq. (35) will be solved to provide the perturbation velocity in the tunnel. As long as the flow remains subcritical everywhere on the airfoil, Eq. (42) can be solved conveniently by a direct iteration process:

$$u_j^n = \hat{u}_j + \frac{(u_j^{n-1})^2}{2} - \sum_{k=1}^{N} \frac{(u_k^{n-1})^2}{2} \epsilon_{jk} j = 1,2,\ldots N\,;\ n = 1,2,.. \tag{43}$$

where the superscript n indicates the nth step in the iteration and $u_j^0 = \hat{u}_j$. However, if the flow becomes supercritical

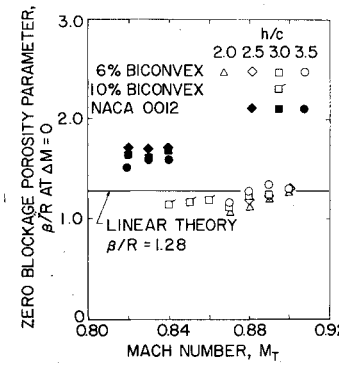

Fig. 9 Porosity parameter required for zero blockage interference.

anywhere on the airfoil, this iteration method fails to converge. For supercritical flows, Eq. (42) is recast in the quadratic form

$$u = I \pm [2I - (2\hat{u} - 1)]^{1/2} \tag{44}$$

where for convenience I represents the influence coefficient series of Eq. (42). The positive sign indicates supersonic flow locally, whereas the negative sign indicates subsonic flow locally. To insure real solutions, the discriminant of Eq. (44) must be positive and to prevent expansion shocks it is required at the sonic point that

$$[2I - (2\hat{u} - 1)]_{\bar{x}_{\text{sonic}}} = 0 \tag{45}$$

and

$$(\partial/\partial\bar{x})[I - \hat{u}]_{\bar{x}_{\text{sonic}}} = 0 \tag{46}$$

An iteration process, developed by Spreiter and Alksne[31] was used to solve Eq. (44) wherein the shock location is held fixed while the reference Mach number is adjusted such that Eqs. (45) and (46) are satisfied at each step of the iteration. Care was exercised to change the sign in Eq. (44) from negative to positive at the location of the sonic point as determined by Eqs. (45) and (46) and to revert back to the negative sign downstream of the prescribed shock location. Deatils of the iterative procedure are given in Ref. 30. The pressure coefficient is found from u as

$$C_P = \{(-2\tau^{2/3}K)/[M_T^{2/3}(\gamma+1)]\}u \tag{47}$$

III. Discussion of Results and Concluding Remarks

To assess the validity of the analytical methods described in the previous section, results from each method have been compared with limited experimental data and results from other theoretical solutions. The results from the LTT method can be used directly to correct wind-tunnel data. Taking a circular-arc airfoil as an example, it is shown in Fig. 3 that the present theoretical correction accounts for the difference between free-air and closed-tunnel solutions. However, as the pressure near the trailing edge of the airfoil has a large gradient which indicates the appearance of a shock wave, the linearized tunnel correction theory is not applicable to the portion of the flow downstream of the shock wave.

One of the advantages of the LTT method is that it can be extended readily to solve for the interference on axisymmetric bodies in circular tunnels. The results of a blockage correction to the experimental pressure distribution over a 20° cone-cylinder model[32] using the LTT method are compared in Fig. 4 with interference-free data of Ref. 33. The perforated tunnel data were obtained on a 1.47% blockage model in a tunnel with variable porosity walls comprised of two plates with inclined holes, one plate sliding relative to the other. Based on a previous study,[34] a value of the porosity parameter, $Q = 0.7$, was assumed to compute the interference. The interference-free data in Fig. 4 were obtained on a 0.0062% blockage model. The agreement after the blockage

correction is satisfactory. It should be noted that the local flow over the cone-cylinder model has not reached supercritical conditions.

To evaluate properly the effect of the perforated walls on shock location requires a nonlinear method such as the IEM. To demonstrate the integral method, a biconvex airfoil and NACA 0012 airfoil were selected to represent typical sharp and blunt leading-edge profiles, respectively. To eliminate the leading-edge singularity of the order of $(\bar{x})^{-1/2}$ for the blunt leading-edge airfoil, the linear solution, $\hat{u}$, was modified by including higher-order terms in the boundary condition.[30] Furthermore, for an airfoil with an essentially constant radius of curvature (such as the sharp leading-edge biconvex airfoil) best agreement with other theories is obtained if the decay parameter, $r(\bar{x})$ is held constant over the airfoil. For blunt leading-edge airfoils with a rapidly varying radius of curvature near the leading edge the decay parameter must vary over the airfoil.

A typical result from the IEM for supercritical flow over a biconvex airfoil is a closed wind tunnel with $h/c=2.07$ is compared in Fig. 5 with the numerical solution of Murman[11] and Laval.[14] The agreement is excellent. Using 20 increments on the airfoil, the IEM solution required approximately 10 sec compared with almost 2 min for Murman's relaxation solution on an IBM 370/165 computer. The time required for the time-dependent method was over two hr on an IBM 360/50 computer. A result from the IEM for flow in a perforated-wall tunnel ($\bar{Q}=0.2$) is shown to agree with the numerical solution of Murman in Fig. 6. The flow over a 6% biconvex airfoil using the IEM is compared in Fig. 7 with the experimental data of Collins and Krupp[35] and again the agreement is excellent. Thus, the nonlinear IEM theory provides an efficient accurate method for determining the flow past a thin airfoil in a perforated wall wind tunnel including shock waves.

A systematic study of the effects of the perforated walls on the shock wave was performed for the 6% biconvex and NACA 0012 airfoils. These results are conveniently summarized in terms of a correction factor, $\Delta M=M_{\text{free-air}}-M_T$, which gives the equivalent free-air Mach number corresponding to the shock location on the airfoil in the tunnel. A typical result for the 6% biconvex airfoil at various porosities is shown in Fig. 8 and shows that at a value of porosity parameter which minimizes the interference at a given Mach number is essentially independent of h/c. A summary of the porosity parameters required for zero blockage interference on the biconvex and NACA 0012 airfoils is given in Fig. 9. The most important observation to be made from Fig. 9 is that the porosity factor required for interference-free testing is dependent on the model. The use of the zero-interference porosity factor for the biconvex airfoil, say $\beta/R=1.2$, can produce an increment in Mach number that could move the shock wave on the NACA 0012 airfoil as much as 10%. Thus, future generation transonic wind tunnels must be able to adjust porosity with Mach number and test configuration to minimize wall interference.

The integral equation method can be extended readily to include lifting airfoils, and the details are given in Ref. 30. However, unlike the linear solution, the effects of thickness and lift cannot be separated because of the nonlinearity of the transonic theory. Furthermore, the extension of the IEM to three-dimensional flows is relatively straightforward, although the simplicity of using an image system to satisfy the wall boundary conditions cannot be extended to three dimensions. However, the efficiency of the IEM could make it advantageous over present three-dimensional numerical methods.

Acknowledgment

The research reported herein was conducted by the Arnold Engineering Development Center, Air Force Systems Command. Research results were obtained by personnel of ARO, Inc., contract operator at AEDC.

References

[1]Pindzola, M. and Lo, C.F., "Boundary Interference at Subsonic Speeds in Tunnels with Ventilated Walls," Arnold Engineering Development Center, Arnold AFB, Tenn., AEDC-TR-69-47 (AD687440), May 1969.

[2]Garner, H.C., Rogers, E.W.E., Acum, W.E.A., and Maskell, E.C., "Subsonic Wind Tunnel Wall Corrections," AGARDograph 109, Oct. 1966.

[3]Murasaki, T., "Sonic Tunnel Wall Interference and Some Other Problems," *Transactions of the Japan Society of Aerospace Sciences,* Vol. 4, 1961, pp. 29-56.

[4]Sandeman, R.J., "On the Application of "Local Linearization" Methods to Choked Wind Tunnel Flow Problems," *Symposium Transsonicum,* Springer-Verlag, Berlin, 1964, pp. 355-361.

[5]Spreiter, J.R., Smith, D.W., and Hyett, B.J. "A Study of the Simulation of Flow with Free-Stream Mach Number 1 in a Choked Wind Tunnel," NASA TR R-73, 1960.

[6]Romberg, G., "Die Stromung im Blockierten Kreiskanal,"- *Symposium Transsonicum,* Springer-Verlag, Berlin, 1964, pp. 345-354.

[7]Goodman, T.R., "A Criterion for Assessing Wind-Tunnel Wall Interference at Mach 1," *Journal of Aircraft,* Vol. 10, Nov. 1973, pp. 695-697.

[8]Berndt, S.B., "Theory of Wall Interference in Transonic Wind Tunnels," *Symposium Transsonicm,* Springer-Verlag, Berlin, 1964, pp. 288-309.

[9]Murman, E.M. and Cole, J.D., "Calculation of Plane Steady Transonic Flows," *AIAA Journal,* Vol. 9, Jan. 1971, pp. 114-121.

[10]Bailey, F.R., "Numerical Calculation of Transonic Flow about Slender Bodies of Revolution," NASA TN D-6582, 1971.

[11]Murman, E.M., "Computation of Wall Effects in Ventilated Transonic Wind Tunnels," AIAA Paper 72-1007, Palo Alto, Calif., Sept. 1972.

[12]Kacprzynski, J.J., "Transonic Flowfield Past 2-D Airfoils Between Porous Wind-Tunnel Walls with Nonlinear Characteristics," *AIAA Journal,* Vol. 14, April 1976, pp. 533-535.

[13]Catheral, D., "The Computation of Transonic Flows Past Aerofoils in Solid, Porous or Slotted Wind Tunnels," *AGARD Symposium on Wind Tunnel Design and Testing Techniques,* Oct. 6-8, 1975, London.

[14]Laval, P., "Methodes Instationnaires de Calcul des Effets d'Interaction de Paroi en Ecoulement Bidimensionnel Supercritique," *La Recherche Aerspatiale,* No. 5, Sept.-Oct. 1973, pp. 273-288.

[15]Laval, P. and Erard, M., "Calcul des Effets de Paroi Permeable en Ecoulement Supercritique," ONERA TN211, 1973.

[16]Newman, P.A. and Klunker, E.B., "Numerical Modelling of Tunnel-Wall and Body-Shape Effects on Transonic Flow Over Finite Lifting Wings," NASA SP 347, 1975, pp. 1189-1212.

[17]Cole, J.D., *Perturbation Methods in Applied Mathematics,* Blaisdell Publishing Co., Waltham, Mass., 1968.

[18]Krupp, U.A., "The Numerical Calculation of Plane Steady Transonic Flows Past Thin Lifting Airfoils," PhD Dissertation, 1971, University of Washington; also Boeing Scientific Research Laboratory Rept. D180-12958-1, June 1971.

[19]Baldwin, B.S., et al., "Wall Interference in Wind Tunnels with Slotted and Porous Boundaries at Subsonic Speeds," NACA TN 2176, May 1954.

[20]Jacocks, J.L., "An Investigation of the Aerodynamic Characteristics of Ventilated Test Section Walls for Transonic Wind Tunnels," PhD Dissertation, University of Tennessee, Knoxville, Tenn., Dec. 1976.

[21]Oswatitsch, K., "Flow Around a Body of Revolution at Mach Number One," *Brooklyn Polytechnic Institute Conference on High Speed Aeronautics,* Brooklyn, N.Y., 1955.

[22]Maeder, P.F. and Wood, A.D., "Linearized Transonic Flows Past Isolated Non-Lifting Airfoils," Brown University, Providence, R.I., TR-WT-24, June 1957.

[23]Spreiter, J.R., "The Local Linearization Method in Transonic Flow Theory," *Symposium Transsonicum,* Springer-Verlag, Berlin, 1964, pp. 152-183.

[24]Lo, C.F., "Application of Linearized Transonic Theory to Tunnel Blockage Interference," Arnold Engineering Development Center, Arnold AFS, Tenn., AEDC-TR-74-65, Sept. 1974.

[25]Hosokawa, I., "A Simplified Analysis for Transonic Flows Around Thin Bodies," *Symposium Transsonicum,* Springer-Verlag, Berlin, 1964, pp. 184-199.

[26]Mokry, M., "Integral Equation Method for Calculation of Subsonic Flow Past Airfoils in a Ventilated Wind Tunnel; Com-

parison with NAE High Reynolds Number Measurements," *AIAA Journal,* Vol. 13, Jan. 1975, pp. 47-55.

[27]Oswatitsch, K., "Die Geschwindigkeitsverteilung bei lokalen Überschallgebieten on flachen Profilen," *Zeitschrift Angewandte Mathemetik und Physik,* Vol. 30, 1950, pp. 17-24.

[28]Norstrud, H., "Numerische Lösungen für Schallnahe Strömungen um ebene Profile," *Zeitschrift fŕr Flugwissenschaften,* Vol. 18, May 1970, pp. 149-157.

[29]Nixon, D., "Calculation of Transonic Flows Using an Extended Integral Equation Method," AIAA Paper 75-876, Hartford, Conn., June 1975; also *AIAA Journal,* to be published.

[30]Kraft, E.M., "An Integral Equation Method for Boundary Interference in Perforated-Wall Wind Tunnels at Transonic Speeds," Ph. D. Dissertation, Dec. 1975, University of Tennessee; also published as AEDC-TR-76-43, April 1976.

[31]Spreiter, J.R. and Alksne, R., "Theoretical Prediction of Pressure Distributions on Nonlifting Airfoils at High Subsonic Speeds," NACA TN 3096, March 1954.

[32]Davis, J.W. and Graham, R.F., "Wind-Tunnel Wall Interference Effects for 20° Cone-Cylinders," *Journal of Spacecraft and Rockets,* Vol. 10, Oct. 1973, pp. 671-678.

[33]Capone, F.J. and Coates, E.M., Jr., "Determination of Boundary-Reflected-Disturbance Lengths in the Langley 16-Foot Transonic Tunnel," NASA TN D-4153, Sept. 1967.

[34]Binion, T. W. and Lo, C. F., "Application of Wall Corrections to Transonic Wind Tunnel Data," AIAA Paper 72-1009, Palo Alto, Calif., Sept. 1972.

[35]Collins, D. J. and Krupp, J. A., "Experimental and Theoretical Investigations in Two-Dimensional Transonic Flow," *AIAA Journal,* Vol. 12, June 1974, pp. 771-778.